

Rate dependence of the tensile and flexural strengths of glass-ceramic Macor

Shiming Dong · Kaiwen Xia · Sheng Huang ·
Tubing Yin

Received: 31 May 2010/Accepted: 19 August 2010/Published online: 1 September 2010
© Springer Science+Business Media, LLC 2010

Abstract Understanding of the tensile and flexural strengths of the glass-ceramic Macor bears important applications in materials science, aerospace, defense, and other engineering disciplines. In this article, we systematically investigate the rate dependence of the tensile strength and the flexural strength of Macor utilizing two methods: the Brazilian disk (BD) test and semi-circular bend (SCB) test. Both static tests and dynamic tests are conducted to explore the rate dependence of tensile and flexural strengths of Macor. The static measurement is conducted with a servo-controlled material testing machine, and the dynamic experiment is carried out with a 6.35-mm diameter split Hopkinson pressure bar (SHPB) system. The pulse-shaping technique is used to achieve dynamic force balance, and thus eliminates the loading inertial effect and enables quasi-static stress analysis. The experimental results show that both the tensile strength and the flexural strength of Macor are loading rate dependent. The flexural strength is observed to be consistently higher than the tensile strength.

Introduction

As a good thermal and electrical insulator, Macor has been extensively used in aerospace, armor design, and other commercial applications. Many applications for ceramic materials are also impact related. Therefore, reliable

material models that can accurately describe the responses of such ceramic materials under dynamic loading conditions are necessary for structural design and optimization purposes.

Various efforts have been invested to develop a better understanding of different aspects in ceramic mechanical properties under both quasi-static and dynamic loading conditions. The experimental investigations of compressive strength under quasi-static loading condition as well as radial confining pressure have been performed on the material test system (MTS) by Chen and Ravichandran [1] and Chen et al. [2]. The results show that the compressive strength increases monotonically from 435 to 485 MPa as lateral confinement increases from 0 to 88 MPa. A modified split Hopkinson pressure bar (SHPB) was used to investigate the dynamic mechanical properties of Macor [1, 3]. The experimental results indicate that the dynamic compressive strength increases from 450 to approximately 1350 MPa as the lateral confining pressure increases from 0 to 230 MPa. Bagdassarov [4] experimentally studied the viscoelastic behavior of Macor and obtained the shear modulus and internal friction of Macor. So et al. [5] used the pulse-echo method to investigate ultrasonic properties of Macor at its cryogenic temperature.

As a typical brittle material, Macor is considerably weaker in tension than in compression. Understanding of tensile strength of Macor is thus of great importance in its engineering applications. Given the fact, the existing studies on the mechanical response of Macor were mainly concerned on its compressive response; it is the objective of this study to investigate the tensile responses of Macor.

Direct tensile or pull test has been a natural approach to measure the tensile strength of solids. However, in practice, the ideal uniform stress state in the specimen is rarely obtained. Therefore, various indirect methods have been

S. Dong · K. Xia (✉) · S. Huang · T. Yin
Department of Civil Engineering, University of Toronto,
Toronto, ON M5S 1A4, Canada
e-mail: kaiwen@ecf.utoronto.ca

S. Dong
College of Architecture and Environment, Sichuan University,
Chengdu, Sichuan 610065, People's Republic of China

employed to measure the tensile strength of brittle materials. These methods aim at generating tensile stress in the sample by far-field compression, which is much easier in instrumentation than direct tensile tests. Among these indirect methods, the diametrical compression of a thin disk specimen, generally referred to as the Brazilian disk (BD) test [6], is probably the most popular one due to its convenience in specimen preparation and experimental implementation. It has been suggested by the American Society for Testing and Materials (ASTM) as a recommended method for tensile strength measurement of brittle solids [7] and, therefore, is first chosen in this study. BD tests have been chosen by many researchers to measure the indirect tensile strength of brittle materials including rocks, ceramics, and concretes [8–11]. Recently, Dai et al. [12, 13] proposed a semi-circular bend (SCB) to measure the dynamic flexural strength of rocks and other brittle materials. The SCB test is chosen in this study to measure the flexural strength of Macor.

It is well known that in those dynamic tests featuring high loading rates, the induced stress in the sample is transient. This results in the loading inertial effect [14]. For dynamic tests, it is commonly believed that it takes several round trips of the stress wave in the sample before the stress reaches an equilibrium state [15, 16]. When the far-field dynamic force balance is satisfied, the inertial effects associated with stress wave loading are minimized, and thus, one can apply the simple quasi-static analysis to obtain the tensile strength in SHPB testing [12]. In order to facilitate dynamic force equilibrium and thus eliminate the inertial effect, the pulse-shaper technique in conventional SHPB tests was proposed [3, 16]. The pulse shaper reduces the slope of the loading pulse and thus allows more time for a compression sample to achieve an almost stress equilibrium state during loading, and thus is adopted in this study.

In this article, we systematically investigate the rate dependence of the tensile strength and the flexural strength of Macor using two methods: BD test and SCB test. The static measurement is conducted with a servo-controlled material testing machine, and the dynamic experiment is carried out with a 6.35-mm SHPB system. The pulse-shaper technique is used to achieve dynamic force balance and thus eliminates the loading inertial effect. It is found that both the tensile strength and flexural tensile strength of Macor exhibit strong rate dependence. The flexural strength is consistently higher than the tensile strength. This may be due to the phenomenon of clustering [17].

Material and specimens

Macor is a white glass ceramic composite comprised of a fluorophlogopite mica phase (55%) interspersed in a

Table 1 Physical properties of Macor [18]

Density	Young's modulus	Shear modulus	Poisson's ratio	Quasi-static compressive strength
2520 kg/m ³	64.1 GPa	25.4 GPa	0.26	345 MPa

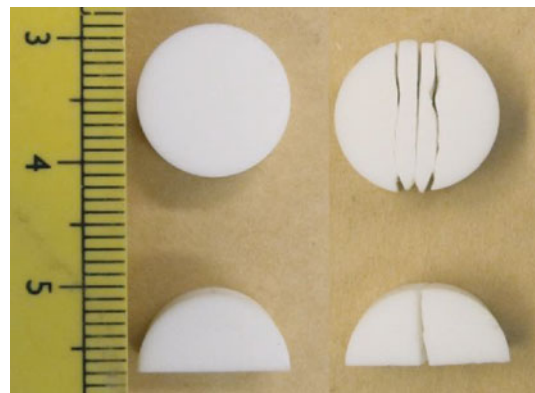


Fig. 1 Photos of BD and SCB specimens: virgin samples on the *left* column and typical tested samples on the *right* column

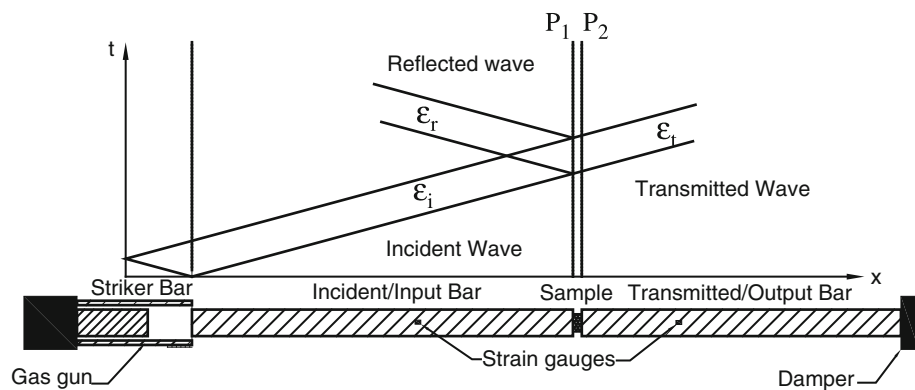
borosilicate glass matrix (45%). The microstructure consists of a network of randomly oriented interlocking 1–2- μm thick mica flakes that are approximately 10 μm in planar dimension parallel to the cleavage basal plane. Some of the relevant physical properties of Macor are listed in Table 1.

Macor used in this research is in the form of rod with a nominal diameter of 13.00 mm. It was then machined and sliced to obtain disks with a diameter of 12.72 mm and an average thickness of 5.57 mm. The SCB specimens are subsequently made from the disks by diametrical cutting (Fig. 1). The typical failed samples are also shown in Fig. 1.

Experimental setup

Static measurement is conducted with an MTS hydraulic servo-control testing system. A constant loading rate of 0.005 mm/s is applied for all the tests. The load is measured with a 50-kN load cell. Dynamic test is conducted using a 6.35-mm SHPB system. It is composed of an 80 mm striker bar, a 600 mm incident bar, and a 400 mm transmitted bar, all made of high strength maraging steel. The specimen is sandwiched between the incident and transmitted bars. Two strain gauges are mounted at 300 and 100 mm away from the bar-sample interfaces on the incident bar and transmission bar, respectively.

Fig. 2 Schematics of a compression split Hopkinson pressure bar and the x - t diagram of stress waves



An eight-channel Sigma digital oscilloscope by Nicolet is used to record and store the strain signals collected from the Wheatstone bridge circuits after amplification.

The impact of the striker bar on the free end of the incident bar induces a longitudinal compressive wave propagating in both left and right directions. The left-propagating wave is fully released at the free end of the striker bar and forms the trailing end of the incident compressive pulse (Fig. 2). Upon reaching the bar–specimen interface, part of the incident wave is reflected (reflected wave) and the remainder passes through the specimen to the transmitted bar (transmitted wave). These three elastic stress pulses in the incident and transmitted bars are recorded with strain gauges glued on the incident and transmitted bars. Assuming one-dimensional stress wave propagation, the forces on both ends of the sample are:

$$P_1 = AE (\varepsilon_i + \varepsilon_r), \quad P_2 = AE \varepsilon_t, \quad (1)$$

where P_1 is the force on the incident end of the specimen, P_2 is the force on the transmitted end. ε is the strain, the subscripts i, r, and t refer to the incident, reflected, and transmitted waves, respectively. A is the cross-sectional area, and E is the Young's modulus of the bars.

A newly developed pulse-shaper technique of SHPB method is utilized. The pulse-shaper technique in SHPB is especially useful for investigating dynamic response of brittle materials such as rocks, glasses, and ceramics [3]. Without proper pulse shaping, it is difficult to achieve dynamic stress equilibrium in such materials because the sample may fail immediately from its end in contact with the incident bar when it is impacted by the incident wave. In the modified SHPB test, we use the C11000 copper as the shaper which was placed at the impact end of the incident bar, to transform the incident wave from a rectangular shape to a ramped shape. During tests, the striker impacts the pulse shaper before the incident bar, thus generating a non-dispersive ramp pulse propagating into the incident bar and, therefore, facilitating the dynamic force balance for the BD and SCB specimens.

Methodologies

BD test

In static testing, the disk sample is compressed diametrically with loading platens in the MTS hydraulic servo-control testing system (Fig. 3), where D and B are the diameter and the thickness of the disk, respectively, and P is the diametrical load. For the dynamic test, the disk specimen in the SHPB system is sandwiched between the incident bar and the transmitted bar.

Under the quasi-static loading condition, $P_1 = P_2 = P$ the tensile stress at the disk center can be expressed as [19]:

$$\sigma_t = \frac{2P(t)}{\pi BD} \quad (2)$$

The tensile strength can be determined by substituting the critical load as the failure occurs into Eq. 2.

Dynamic Brazilian tests were carried out on a modified SHPB setup. A typical set of the incident, reflected, and transmitted signals from a dynamic BD test are shown in Fig. 4. The rising time is about 40 μ s, and the pulse width is about 80 μ s. In order to check whether the force balance is achieved between both ends of the specimen, we compare the time-varying forces on both ends of the specimen for a typical dynamic Brazilian test with pulse shaping in SHPB. The dynamic forces on both sides of the specimen

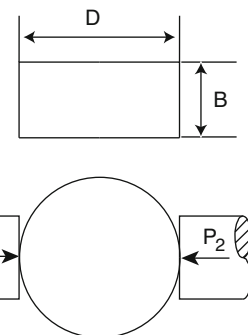


Fig. 3 Schematics of the BD specimen assembly

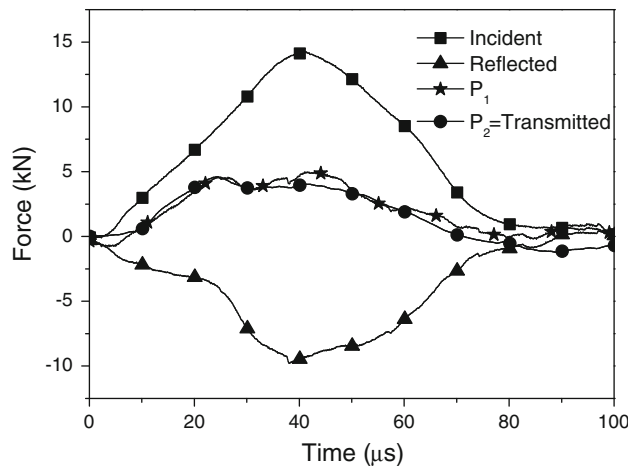


Fig. 4 Dynamic force balance check for a typical dynamic BD test

are almost identical before the critical failure point is reached during dynamic loading. It is obvious that the transmitted force increases approximately linearly with time. The loading rate of the tensile test can thus be determined with Eq. 2 by fitting the slope of the loading. The loading rate was nearly constant during the loading stage of the test, which is important when the strength results need to be reported as a function of loading rates [20].

For dynamic Brazilian tests, dynamic force balance on both ends of the specimen is achieved, and thus, Eq. 2 can be used to calculate the dynamic tensile strength. We only need to replace the static loading history in Eq. 2 with the dynamic loading history determined from the stress wave analysis.

SCB test

The SCB method can be viewed as an integration of the Brazilian disk and the conventional three-point bending methods using one-dimensional sample with circular or rectangular cross section. The loading configuration of the SCB in both MTS hydraulic servo-control testing system and SHPB system is schematically shown in Fig. 5, where R is the radius of the half disk, and B is the thickness of the ceramic disk. The span between the two supporting pins is S . Upon loading, failure will be initiated at the failure spot O , the center of the original disk.

In quasi-static case, the equation for calculating the tensile stress at O is [12]:

$$\sigma(t) = \frac{P(t)}{\pi BR} Y(S/2R) \quad (3)$$

where $P(t)$ is the time-varying load recorded in the test. The dimensionless stress $Y(S/2R)$ is a function of dimensionless distance $S/2R$ and can be expressed as [12]:

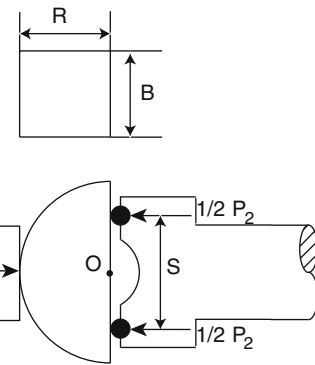


Fig. 5 Schematics of the SCB specimen assembly

$$Y = 2.22 + 2.87 \left(\frac{S}{2R} \right) + 4.54 \left(\frac{S}{2R} \right)^2 \quad (4)$$

For the fixed geometry of the SCB sample used in this research ($2R = 12.72$ mm, $B = 5.57$ mm, and $S = 9.525$ mm), Y is equal to 6.916.

Dynamic SCB tests are carried out on a modified SHPB setup. The curved end of the specimen is in tangential contact with the incident bar, and the flat end is in contact with the transmitted bar through two supporting pins separated also by the same distance S as in static SCB tests.

For static tests, the flexural tensile strength, $P(t) = P$, can be determined by substituting the critical load as failure occurs into Eq. 3. For dynamic SCB tests, the modified SHPB system with proper pulse shaping is employed to ensure dynamic force balance on both ends of the specimen, and thus, Eq. 3 can be used to calculate the dynamic flexural tensile strength. To ensure force balance on the SCB specimen, we compare the time-varying forces on both ends of the specimen for a typical dynamic SCB test with pulse shaping in SHPB (Fig. 6). It can be seen that the dynamic forces on both sides of the specimen are almost identical before the critical failure point is reached. It is also obvious that the transmitted force increases almost linearly with time during the loading. We only need to replace the static loading history in Eq. 3 with the dynamic loading history determined from the stress wave analysis and obtain the loading rate by fitting for the slope of the loading.

Results and discussion

Brazilian testing

The typical fracture pattern shown in (Fig. 1) demonstrates that the BD test is valid [7]. The average tensile strength obtained from three specimens was 26 MPa with the average loading rate of 2.64×10^{-4} GPa/s on the Macor

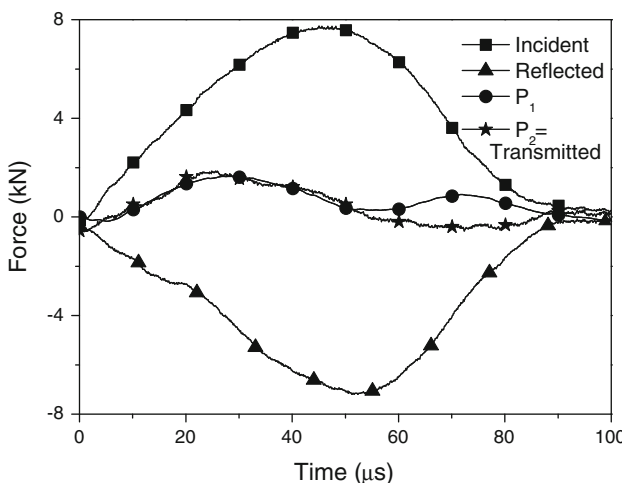


Fig. 6 Dynamic force balance check for a typical dynamic SCB test

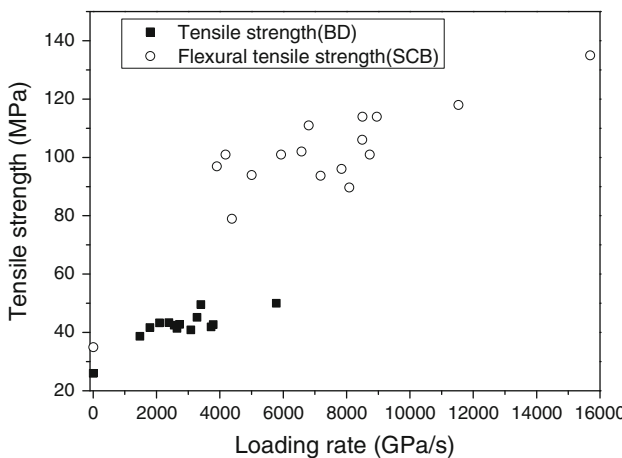


Fig. 7 Variation of strengths of Macor with the loading rate

material used in this research, which is about 10% of the compressive strength quoted by the manufacturer (see Table 1). The dynamic tensile strengths are obtained at loading rates ranging from 1476 to 5780 GPa/s. The maximum dynamic tensile strength is 50 MPa with the loading rate of 5780 GPa/s, which is almost twice as high as the static tensile strength of 26 MPa. The variation in tensile strength as a function of loading rate for the Brazilian test is illustrated in Fig. 7.

SCB testing

A straight crack is produced from the failure point along the loading axis (Fig. 1), which split the SCB specimen into two halves. The average flexural tensile strength obtained from three specimens was 35 MPa with an average loading rate of 5.86×10^{-4} GPa/s on the Macor material used in this research. The dynamic flexural tensile strengths are obtained at loading rates ranging from 3902

to 15690 GPa/s. The maximum dynamic flexural tensile strength is 135 MPa at a loading rate of 15690 GPa/s, which is almost four times as high as the static flexural tensile strength of 35 MPa. The variation in flexural tensile strength as a function of the loading rate for the SCB test is also illustrated in Fig. 7.

It is evident from Fig. 7 that both the measured tensile strengths and flexural tensile strength of Macor increase with the loading rates. In addition, the flexural tensile strength is consistently higher than the tensile strength.

Discussion

Dai et al. [13] used the SCB test to study on the flexural tensile strength of Laurentian granite under both quasi-static and dynamic loading conditions. The experimental results show that the flexural tensile strength measured from the SCB test has a higher value than the tensile strength measured using the BD method under similar loading rates. Similar results have been observed by Zhao and Li [9]. A non-local theory was used by Dai et al. [13] to rationale the difference between the tensile strength and flexural strength.

The non-local theory depicts that the brittle material will not fail when the tensile strength is exceeded locally; the failure occurs only when the average stress over a characteristic length along the failure path reaches the tensile strength. For a brittle material under uniform tensile loading, the average stress is the same as the local stress, and the non-local failure theory reduces to the traditional strength theory. When there is a stress gradient along the failure path, the average stress will be much smaller than the maximum stress where the failure initiates. The flexural strength measured in this study using the SCB method represents the maximum stress where failure initiates; it is thus larger than the material tensile strength, which is the average stress over the characteristic length along the failure path. A characteristic length of 2.5 mm was used in the non-local theory to explain the gap [13]. For rocks, the grain size is about 1 mm, and thus, the physical meaning of the characteristic length is understandable. To explain the difference between the tensile strength and flexural strength of Macor, the characteristic length will be close to 1 mm, which is substantially larger than its grain size of microns. The well-known phenomenon of clustering [17] may be the solution to this apparent paradox.

Conclusions

Quasi-static and dynamic tensile strength experiments were conducted on Macor with the Brazilian test and SCB test methods. The static tests were conducted with an MTS

hydraulic servo-control testing system, and the Dynamic tests were carried out on a modified SHPB setup.

A pulse-shaping technique was used to achieve dynamic force balance on both ends of the specimen. The experimental results show that both the tensile strength and flexural tensile strength of Macor samples exhibit strong rate dependence and the flexural tensile strength is consistently higher than the tensile strength under both quasi-static and dynamic loading conditions. The difference between the tensile strength and flexural strength may be due to the clustering phenomenon.

Acknowledgement This study was supported by the Natural Sciences and Engineering Research Council of Canada (NSERC) through Discovery Grant No. 72031326, and the National Foundation of Broad Study of China.

References

1. Chen WN, Ravichandran G (1997) J Mech Phys Solids 45:1303
2. Chen WW, Rajendran AM, Song B, Nie X (2007) J Am Ceram Soc 90:1005
3. Frew DJ, Forrestal MJ, Chen W (2002) Exp Mech 42:93
4. Bagdassarov NS (1999) Phys Chem Miner 26:513
5. So JH, Green DH, Yun SS (2003) J Mater Sci 38:2007. doi:[10.1023/A:1023593506454](https://doi.org/10.1023/A:1023593506454)
6. Mellor M, Hawkes I (1971) Eng Geol 5:173
7. ASTM C1144-89 (2004) Annual book of ASTM standards. ASTM International
8. Chen CS, Pan E, Amadei B (1998) Int J Rock Mech Min Sci 35:43
9. Zhao J, Li HB (2000) Int J Rock Mech Min Sci 37:861
10. Johnston C, Ruiz C (1995) Int J Solids Struct 32:2647
11. Gomez JT, Shukla A, Sharma A (2001) Theor App Fract Mech 36:37
12. Dai F, Xia K, Luo SN (2008) Rev Sci Instrum 79:123903
13. Dai F, Xia KW, Tang LZ (2010) Int J Rock Mech Min Sci 47:469
14. Bohme W, Kalthoff JF (1982) Int J Fract 20:R139
15. Dong SM, Wang Y, Xia YM (2006) Polym Test 25:943
16. Song B, Chen W (2004) Exp Mech 44:622
17. Kendall K, Alford NM, Clegg WJ, Birchall JD (1989) Nature 339:130
18. Corning Incorporated (1992) Technical Bulletin, New York
19. Bieniawski ZT, Hawkes I (1978) Int J Rock Mech Min Sci 15:99
20. Nie X, Chen WNW, Wereszczak AA, Templeton DW (2009) J Am Ceram Soc 92:1287